General quantum constraints on detector noise in continuous linear measurements

Miao, Haixing

DOI:
10.1103/PhysRevA.95.012103

Document Version
Peer reviewed version

Citation for published version (Harvard):
Miao, H 2017, 'General quantum constraints on detector noise in continuous linear measurements', *Physical Review A - Atomic, Molecular, and Optical Physics*, vol. 95, 012103.
https://doi.org/10.1103/PhysRevA.95.012103

General quantum constraints on detector noise in continuous linear measurement

Haixing Miao[1]

[1]*School of Physics and Astronomy, University of Birmingham, Birmingham, B15 2TT, United Kingdom*

In quantum sensing and metrology, an important class of measurement is the continuous linear measurement, in which the detector is coupled to the system of interest linearly and continuously in time. One key aspect involved is the quantum noise of the detector, arising from quantum fluctuations in the detector input and output. It determines how fast we acquire information about the system, and also influences the system evolution in terms of measurement back action. We therefore often categorize it as the so-called imprecision noise and quantum back action noise. There is a general Heisenberg-like uncertainty relation that constrains the magnitude of and the correlation between these two types of quantum noise. The main result of this paper is to show that when the detector becomes ideal, i.e., at the quantum limit with minimum uncertainty, not only does the uncertainty relation takes the equal sign as expected, but also there are two new equalities. This general result is illustrated by using the typical cavity QED setup with the system being either a qubit or a mechanical oscillator. Particularly, the dispersive readout of qubit state, and the measurement of mechanical motional sideband asymmetry are considered.

I. INTRODUCTION AND SUMMARY

When we probe classical signals or quantum systems, noise in the detector limits our ability to extract the relevant information. If the classical noise is sufficiently suppressed, the detector will enter the regime where intrinsic quantum fluctuations in its degrees of freedom determines the statistical property of the noise. Modern experiments are approaching such a quantum-noise-limited regime [1, 2]. The state-of-the-art includes, e.g., high-fidelity qubit readout [3], gravitational-wave detection using laser interferometers [4, 5], and quantum optomechanics in general [6, 7].

In the quantum regime, those experiments mentioned above can be modeled as the continuous linear quantum measurement, which is represented schematically in Fig. 1. The system can be, e.g. either a qubit or a mechanical oscillator, which can be further attached to a classical signal if acting as a sensor. The detector is a quantum field that contains many degrees of freedom, e.g. the optical field in optomechanics, and interacts with the system continuously in time. We call the degree of freedom linearly coupled to the system variable $\hat{q}$ as the input port with its observable denoted by $\hat{F}$, which, e.g. in optomechnaics, is the force acting on the mechanical oscillator; the output port with observable $\hat{Z}$ is the one projectively measured by a macroscopic device (e.g. the photodiode) that produces classical data.

The determining factor behind different measurement tasks is the quantum noise, arising from quantum fluctuations in the detector input and output ports. Particularly, the output-port fluctuation gives rise to the so-called imprecision noise that quantifies how well we can probe the system in terms of measurement precision and rate; the input-port fluctuation perturbs the system and leads to the quantum back action noise, which, in the case of a qubit, can induce dephasing. If the quantum noise at different times is not correlated, one can use the master equation approach to study decoherence of the system or quantum-trajectory approach for analyzing the system evolution conditional on the measurement outcome (see, e.g., Ref. [8] or Chapter 4 in Ref. [9]).

An alternative approach that can treat general correlated quantum noise is the linear-response theory developed by Kubo, and is summarized in his seminal paper on the fluctuation-dissipation theorem [10]. Averin applied it to the dispersive quantum non-demolition measurement (QND) of a qubit [11, 12], which has been further elaborated by Clerk *et al.* [13] and also extensively reviewed in Ref. [1]. Braginsky and Khalili applied this approach to study the sensitivity of quantum-limited force/displacement sensors [14]. In this approach, different dynamical quantities are related by the susceptibility function χ which describes the linear response. The statistical property of the quantum noise is quantified by the two-time correlation function, or equivalently, the frequency-domain noise spectral density (spectrum) $\bar{S}$ for time-invariant (stationary) detectors.

At thermal equilibrium, the spectral density and susceptibility are connected by the famous fluctuation-dissipation theorem [10, 15]. In contrast, the measurement process considered here is far away from the thermal equilibrium. Nevertheless, there is a general Heisenberg-like uncertainty relation connecting them, which constrains the imprecision noise and quantum back action noise of the detector, even without knowing details of the system. According to Ref. [14], such a relation can be written explicitly as[‡]:

$$\bar{S}_{ZZ}(\omega)\bar{S}_{FF}(\omega) - |\bar{S}_{ZF}(\omega)|^2 \geq (\hbar^2/4)|\chi_{ZF}(\omega)|^2 + \hbar\big|\Im[\bar{S}^*_{ZF}(\omega)\chi_{ZF}(\omega) - \chi_{FF}(\omega)\bar{S}_{ZZ}(\omega)]\big|. \quad (1)$$

Here the spectral densities $\bar{S}_{ZZ}(\omega)$ and $\bar{S}_{FF}(\omega)$ quantifies the magnitude of the imprecision noise and the back action noise at frequency ω, respectively; $\bar{S}_{ZF}$ quantifies the cross correlation; the susceptibility χ_{ZF} describes the response of the

FIG. 1. A schematics for the continuous linear measurement.

[‡] there is a minor typo in [14] concerning the sign in front of χ_{FF}.

detector output to the system variable; the input susceptibility χ_{FF} quantifies the dynamical back action that modifies the system dynamics, which will be illustrated later using a concrete example; $\Im[\cdot]$ means taking the imaginary part. The mathematical definitions for χ and $\bar{S}$ will be given in Eqs. (10) and (13). Note that an uncertainty relation similar to Eq. (1) is also presented in Ref. [1]; however, χ_{FF} has not been included, and this makes the resulting uncertainty relation less tight, especially when $\bar{S}_{ZF}/\chi_{ZF}$ becomes imaginary.

Applying the above uncertainty relation to measurements of different systems, one can arrive at some general principles, regardless of the specific detector used. For example, in the QND measurement of a qubit, $\bar{S}_{ZZ}$ determines the measurement rate $\Gamma_{\rm meas}$ for acquiring information of the qubit state, and $\bar{S}_{FF}$ sets the dephasing rate Γ_ϕ. Eq. (1) leads to a fundamental quantum limit to the measurement rate: $\Gamma_{\rm meas} \le \Gamma_\phi$—we can measure the qubit at most as fast as we dephase it [1, 11–13, 16]. In the classical force/displacement sensing with a quantum mechanical oscillator, Eq. (1) implies a tradeoff between the imprecision noise and the back-action noise, which gives rise to the famous Standard Quantum Limit [14]. Achieving the quantum limit requires the detector to be ideal, i.e., having minimum uncertainty—the thermal excitation of the detector degrees of freedom and other decoherence effects become negligible. There are ongoing experimental efforts towards this goal, e.g., the most recent results with optomechanical devices presented in Refs. [17–20].

The main result presented in this paper is to show that when the detector is at the quantum limit with minimum uncertainty, not only do we have Eq. (1) attain the equal sign, but also obtain two new equalities shown in Eqs. (24) and (25). By introducing $\hat{z} \equiv \hat{Z}/\chi_{ZF}$ normalized by the output response, they can be putted into the following more suggestive form:

$$\bar{S}_{zz}(\omega)\bar{S}_{FF}(\omega) - |\bar{S}_{zF}(\omega)|^2 = \frac{\hbar^2}{4}\,, \tag{2}$$

$$\Im[\bar{S}_{zF}(\omega)] = -\Im[\chi_{FF}(\omega)]\bar{S}_{zz}(\omega)\,. \tag{3}$$

The first equality constraints the strength of the imprecision noise and the back-action noise, while the second one relates the cross correlation $\bar{S}_{zF}$ to the dynamical back action quantified by χ_{FF}. The details will be provided in section III.

To illustrate implications of Eqs. (2) and (3), in section IV, they will be applied to the typical cavity QED setup, in which a cavity mode is coupled to either a qubit or a mechanical oscillator. The key messages are summarized as follows. In the case of dispersive QND qubit readout, there is an optimal output observable such that $\bar{S}_{zF} = 0$, which leads to

$$\Gamma_{\rm meas} = \Gamma_\phi\,. \tag{4}$$

In the case of measuring a mechanical oscillator, the motional sideband asymmetry reported in several experiments [21–25] is considered. One interpretation behind the observed asymmetry is attributing it to the imprecision-back-action noise correlation $\bar{S}_{zF}$ [22, 26]. In particular, near the mechanical resonant frequency ω_m, $\bar{S}_{zF}$ is purely imaginary and

$$\bar{S}_{zF}(\omega_m) \approx \pm i\hbar/2\,, \tag{5}$$

where $\pm$ depends on the detuning frequency of the laser with respect to the cavity resonance. From Eqs. (2) and (3), such a correlation implies

$$\Im[\chi_{FF}(\omega_m)] \approx \mp \bar{S}_{FF}(\omega_m)/\hbar\,. \tag{6}$$

Firstly, this indicates that the noise spectra for the positive and negative frequencies are highly unbalanced, cf., Eq. (15), which is the case in these experiments. Secondly, since χ_{FF} quantifies the dynamical back action to the mechanical oscillator [27–29], the sideband asymmetry observed with the linear measurement is always accompanied by additional heating or damping of the mechanical motion.

The outline of this paper goes as follows: in section II, a brief introduction to the continuous linear measurement is provided. Additionally, the formal definitions for the susceptibility function and the noise spectral density are given; in section III, the derivation of the general quantum constraints on detector noise—Eqs. (2) and (3) is presented; in section IV, these constraints are illustrated with the examples of quantum measurements in the cavity QED setup; in section V, there will be some discussions about extending the result to more general cases.

II. CONTINUOUS LINEAR MEASUREMENT

We now go through the mathematical description of the continuous linear measurement, and define relevant quantities, which follows Refs. [1, 14, 27]. Specifically, the free Hamiltonian $\hat{H}_{\rm det}$ of the detector only involves linear or quadratic functions of canonical coordinates of which the commutators are classical numbers. The system-detector interaction $\hat{H}_{\rm int}$ is in the bilinear form:

$$\hat{H}_{\rm int} = -\hat{q}\,\hat{F}\,. \tag{7}$$

Solving the Heisenberg equation of motion leads to the following solution to the detector observables:

$$\hat{Z}(t) = \hat{Z}^{(0)}(t) + \int_{-\infty}^{+\infty} {\rm d}t'\chi_{ZF}(t-t')\,\hat{q}(t')\,, \tag{8}$$

$$\hat{F}(t) = \hat{F}^{(0)}(t) + \int_{-\infty}^{+\infty} {\rm d}t'\chi_{FF}(t-t')\,\hat{q}(t')\,, \tag{9}$$

where superscript (0) denotes evolution under the free Hamiltonian $\hat{H}_{\rm det}$. The susceptibility χ_{AB}, quantifying the detector response to the system variable $\hat{q}$, is defined as

$$\chi_{AB}(t-t') \equiv (i/\hbar)[\hat{A}^{(0)}(t), \hat{B}^{(0)}(t')]\Theta(t-t')\,, \tag{10}$$

where Θ is the Heaviside function and $\hat{H}_{\rm det}$ is assumed to be time-independent (time-invariant) so that χ_{AB} is a function of the time difference $t-t'$. Note that χ_{AB} is not an operator but a classical number, and it only depends on the free evolution of the detector; both features are attributable to the detector being linear. Moving into the frequency domain, we can relate the susceptibility to the spectral density [1]:

$$\chi_{AB}(\omega) - \chi^*_{BA}(\omega) = (i/\hbar)[S_{AB}(\omega) - S_{BA}(-\omega)]\,. \tag{11}$$

Here S_{AB} is unsymmetrized spectral density defined through

$$\mathrm{Tr}[\hat{\rho}_{\mathrm{det}}\hat{A}^{(0)}(\omega)\hat{B}^{(0)}(\omega')] \equiv 2\pi S_{AB}(\omega)\delta(\omega-\omega'), \quad (12)$$

where $\hat{\rho}_{\mathrm{det}}$ is the density matrix of the detector initial state, the Fourier transform $f(\omega) \equiv \int_{-\infty}^{+\infty} \mathrm{d}t\, e^{i\omega t} f(t)$, and $\mathrm{Tr}[\hat{\rho}_{\mathrm{det}}\hat{A}^{(0)}] = \mathrm{Tr}[\hat{\rho}_{\mathrm{det}}\hat{B}^{(0)}] = 0$ is assumed without loss of generality. The symmetrized version of S_{AB}, quantifying the fluctuation, is

$$\bar{S}_{AB}(\omega) \equiv [S_{AB}(\omega) + S_{BA}(-\omega)]/2. \quad (13)$$

One special case is when $\hat{A}$ and $\hat{B}$ are identical, which leads to Kubo's formula, using $\hat{A} = \hat{B} = \hat{F}$ as an example:

$$\Im[\chi_{FF}(\omega)] = [S_{FF}(\omega) - S_{FF}(-\omega)]/(2\hbar), \quad (14)$$

which quantifies the dissipation. In the thermal equilibrium, $S_{FF}(\omega)$ and $S_{FF}(-\omega)$ differ from each other by the Boltzmann factor $e^{\hbar\omega/(k_B T)}$ with T being temperature, and $\bar{S}_{FF}(\omega)$ is thus related to $\Im[\chi_{FF}(\omega)]$ by the fluctuation-dissipation theorem. For the measurement process far from thermal equilibrium, we generally have

$$\bar{S}_{FF}(\omega) \geq \hbar|\Im[\chi_{FF}(\omega)]|, \quad (15)$$

in which the equal sign is achieved when either $S_{FF}(\omega)$ or $S_{FF}(-\omega)$ vanishes [14]. This relation constraints the quantum fluctuation in either $\hat{Z}$ or $\hat{F}$ individually; the uncertainty relation Eq. (1) connects both together.

III. THE GENERAL QUANTUM CONSTRAINTS

After defining key quantities, we come to the derivation of Eq. (1) and the main result Eqs. (2) and (3)—the general quantum constraints on detector noise. It follows the standard approach outlined in Ref. [14], but uses unsymmetrized spectral density as the starting point, which allows directly showing the condition for achieving the quantum limit. Define the following auxiliary operator:

$$\hat{Q} \equiv \int_{-\infty}^{+\infty} \mathrm{d}\omega[\alpha^*(\omega)\hat{Z}^{(0)}(\omega) + \beta^*(\omega)\hat{F}^{(0)}(\omega)], \quad (16)$$

where α, β are some functions. The norm of $\hat{Q}$ is positive definite, i.e., $||\hat{Q}||^2 \equiv \mathrm{Tr}[\hat{\rho}_{\mathrm{det}}\hat{Q}\hat{Q}^\dagger] \geq 0$, which, in terms of unsymmetrized spectral density, reads

$$\int_{-\infty}^{+\infty} \mathrm{d}\omega\, [\alpha^*, \beta^*] \begin{bmatrix} S_{ZZ}(\omega) & S_{ZF}(\omega) \\ S_{ZF}^*(\omega) & S_{FF}(\omega) \end{bmatrix} \begin{bmatrix} \alpha \\ \beta \end{bmatrix} \geq 0. \quad (17)$$

It needs to be satisfied for arbitrary α and β, which implies

$$S_{ZZ}(\omega)S_{FF}(\omega) - |S_{ZF}(\omega)|^2 \geq 0. \quad (18)$$

Using Eqs. (11) and (13), we can rewrite it as

$$\{\bar{S}_{ZZ}(\omega) \pm \hbar\Im[\chi_{ZZ}(\omega)]\}\{\bar{S}_{FF}(\omega) \pm \hbar\Im[\chi_{FF}(\omega)]\} \geq \left|\bar{S}_{ZF}(\omega) \pm \frac{\hbar}{2i}[\chi_{ZF}(\omega) - \chi_{FZ}^*(\omega)]\right|^2. \quad (19)$$

Here $\pm$ comes from that Eq. (18) needs to be satisfied for both positive and negative frequencies.

In order for $\hat{F}$ and $\hat{Z}$ to be the input and output observables of the detector, the susceptibilities cannot take arbitrary value. Because the macroscopic device, illustrated in Fig. 1, needs to make projective measurement of $\hat{Z}$ continuously in time, which produces a classical data stream. This means the final $\hat{Z}$ after interacting with the system, shown in Eq. (8), can be precisely measured at different times, which happens only if

$$[\hat{Z}(t), \hat{Z}(t')] = 0 \quad \forall t, t'. \quad (20)$$

In Ref. [27], the authors called this as the condition of simultaneous measurability, and further showed that it implies $[\hat{Z}^{(0)}(t), \hat{Z}^{(0)}(t')] = [\hat{F}^{(0)}(t), \hat{Z}^{(0)}(t')]\Theta(t-t') = 0$, i.e.,

$$\chi_{ZZ}(\omega) = \chi_{FZ}(\omega) = 0. \quad (21)$$

Taking this into account, Eq. (19) leads to

$$\bar{S}_{ZZ}(\omega)\bar{S}_{FF}(\omega) - |\bar{S}_{ZF}(\omega)|^2 \geq \frac{\hbar^2}{4}|\chi_{ZF}(\omega)|^2 \pm \hbar\Im[\bar{S}_{ZF}^*(\omega)\chi_{ZF}(\omega) - \chi_{FF}(\omega)\bar{S}_{ZZ}(\omega)]. \quad (22)$$

Since the inequality has to be valid for both plus sign and minus sign in front of $\hbar\Im[\cdot]$, it becomes equivalent to the uncertainty relation Eq. (1).

When the detector is at the quantum limit, Eq. (18) takes the minimum, i.e.,

$$\{S_{ZZ}(\omega)S_{FF}(\omega) - |S_{ZF}(\omega)|^2\}_{\mathrm{quantum\,limit}} = 0. \quad (23)$$

Equivalently, this gives rise to two equalities for either plus sign or minus sign in Eq. (22). Taking their sum and difference, we obtain

$$\bar{S}_{ZZ}(\omega)\bar{S}_{FF}(\omega) - |\bar{S}_{ZF}(\omega)|^2 = \frac{\hbar^2}{4}|\chi_{ZF}(\omega)|^2, \quad (24)$$

$$\Im[\bar{S}_{ZF}^*(\omega)\chi_{ZF}(\omega) - \chi_{FF}(\omega)\bar{S}_{ZZ}(\omega)] = 0, \quad (25)$$

which are reduced to Eqs. (2) and (3) after normalizing $\hat{Z}$ by the susceptibility χ_{ZF}.

One can show explicitly that the quantum limit is achieved when the detector is in the pure, stationary, Gaussian state—the multi-mode squeezed state (see, e.g., Ref. [30]):

$$|\xi\rangle \equiv \exp\left\{\int_0^{+\infty} \frac{\mathrm{d}\omega}{2\pi}[\xi(\omega)\hat{d}^\dagger(\omega)\hat{d}^\dagger(-\omega) - \mathrm{h.c.}]\right\}|0\rangle. \quad (26)$$

Here we have used the fact that the detector is linear with its canonical coordinates having classical-number commutators, and thus it can be modelled as a collection of bosonic modes (bosonic field); $\hat{d}(\omega)$ is the corresponding annihilation operator of the detector mode at frequency ω; $\xi(\omega)$ describes the squeezing factor at different frequencies; h.c. denotes Hermitian conjugate; $|0\rangle$ is the vacuum state. In quantum optics, the zero frequency in Eq. (26) coincides with one half of the pump frequency of the optical parametric oscillator that produces the squeezed state.

Using the fact that $\hat{Z}^{(0)}(t)$ and $\hat{F}^{(0)}(t)$ are Hermitian, we can rewrite their Fourier transform in terms of $\hat{d}(\omega)$ and $\hat{d}^\dagger(-\omega)$:

$$\hat{Z}^{(0)}(\omega) = \mathscr{Z}(\omega)\hat{d}(\omega) + \mathscr{Z}^*(-\omega)\hat{d}^\dagger(-\omega)\,, \quad (27)$$

$$\hat{F}^{(0)}(\omega) = \mathscr{F}(\omega)\hat{d}(\omega) + \mathscr{F}^*(-\omega)\hat{d}^\dagger(-\omega)\,, \quad (28)$$

with some coefficients $\mathscr{Z}$ and $\mathscr{F}$. One can then find that

$$\det\begin{bmatrix} \langle\xi|\hat{Z}(\omega)\hat{Z}^\dagger(\omega')|\xi\rangle & \langle\xi|\hat{Z}(\omega)\hat{F}^\dagger(\omega')|\xi\rangle \\ \langle\xi|\hat{F}(\omega)\hat{Z}^\dagger(\omega')|\xi\rangle & \langle\xi|\hat{F}(\omega)\hat{F}^\dagger(\omega')|\xi\rangle \end{bmatrix} = 0\,, \quad (29)$$

where the superscript (0) is omitted. This is equivalent to Eq. (23) according to the definition of the spectral density shown in Eq. (12).

IV. APPLICATION TO CAVITY QED

To illustrate the above result, let us look at the cavity QED setup shown schematically in Fig. 2. The system can either be a qubit or a mechanical oscillator. The detector consists of a single cavity mode $\hat{a}$ and external continuum field $\hat{c}_x$ with the central frequency defined by the laser frequency ω_l which can be detuned from the cavity resonant frequency ω_r. Its Hamiltonian in the rotating frame of the laser frequency is given by (see, e.g., section 2 in [6])

$$\hat{H}_{\rm det} = \hbar(\omega_r - \omega_l)\hat{a}^\dagger\hat{a} - i\hbar\int_{-\infty}^{+\infty} {\rm d}x\,\hat{c}_x^\dagger\frac{\partial\hat{c}_x}{\partial x} + i\hbar\sqrt{2\gamma}(\hat{a}^\dagger\hat{c}_{x=0} - \hat{a}\hat{c}_{x=0}^\dagger)\,. \quad (30)$$

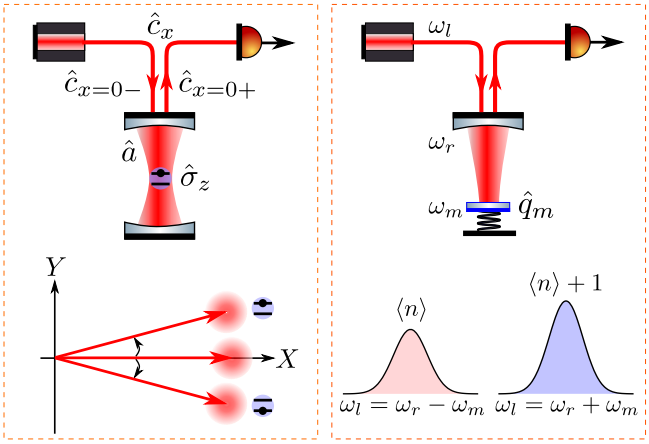

FIG. 2. Schematics for the dispersive qubit readout (left) in which the state-dependent phase shift is inferred by probing the phase quadrature $\hat{Y}$ of the cavity mode, and the sideband asymmetry measurement (right) in which we tune the laser frequency to selectively measure the Stokes and anti-Stokes sidebands scattered by the mechanical motion. In both cases, the cavity mode $\hat{a}$ is continuously driven by the external field $\hat{c}_x$, which contains both the coherent amplitude and quantum fluctuation. We use $\hat{c}_{x=0-}$ ($\hat{c}_{x=0+}$) to denote the ingoing (outgoing) field right before (after) interacting with the cavity mode. The outgoing part is monitored by a photodiode using homodyne detection.

Here subscript x in $\hat{c}_x$ labels the field degree of freedom at different locations; $\hat{c}_{x=0}$ denotes the one directly coupled to the cavity mode at a rate γ. This is the same Hamiltonian for a one-sided cavity in the standard input-output (has a different meaning from the one used here) formalism [31].

The interaction Hamiltonian in two cases, with the system to be a qubit (dispersive-coupling regime [32, 33]) and a mechanical oscillator (optomechanical coupling [6, 7]), are

$$\hat{H}_{\rm int}^{\rm qubit} = -\hbar\frac{g_0^2}{\omega_l - \omega_{01}}\hat{\sigma}_z\hat{a}^\dagger\hat{a}\,, \quad \hat{H}_{\rm int}^{\rm mech} = -\hbar\frac{\omega_r}{L}\hat{q}_m\hat{a}^\dagger\hat{a}\,, \quad (31)$$

where g_0 is the cavity-qubit coupling rate in the Jaynes-Cummings model, ω_{01} is the transition frequency between two energy levels, $\hat{\sigma}_z$ is the Pauli operator, L is the cavity length, and $\hat{q}_m$ is the position of the mechanical oscillator.

For both cases, the input observable $\hat{F}$ is proportional to the cavity photon number $\hat{n}_{\rm cav} = \hat{a}^\dagger\hat{a}$ by comparing with Eq. (7), and thus in general we can write $\hat{F} = \hbar g\hat{n}_{\rm cav}$ with g depending on the specific system. Due to pumping from the laser, the mean cavity photon number $\bar{n}_{\rm cav}$ is much larger than one. The standard approach is linearizing $\hat{n}_{\rm cav}$ and keeping the perturbed part that is proportional to the amplitude quadrature $\hat{X} \equiv (\hat{a} + \hat{a}^\dagger)/\sqrt{2}$. The resulting linearized $\hat{F}$ reads

$$\hat{F} = \hbar g\sqrt{2\bar{n}_{\rm cav}}\hat{X} \equiv \hbar\bar{g}\hat{X}\,. \quad (32)$$

Additionally, given homodyne detection of the outgoing field $\hat{c}_{x=0+}$, the output observable $\hat{Z}$ can be written as

$$\hat{Z} = \cos\theta\,\hat{X}_{\rm out} + \sin\theta\,\hat{Y}_{\rm out}\,, \quad (33)$$

where θ depends on the phase of the local oscillator in the homodyne detection, $\hat{X}_{\rm out} \equiv (\hat{c}_{x=0+} + \hat{c}_{x=0+}^\dagger)/\sqrt{2}$ and $\hat{Y}_{\rm out} \equiv (\hat{c}_{x=0+} - \hat{c}_{x=0+}^\dagger)/(\sqrt{2}i)$ are the amplitude quadrature and phase quadrature of the outgoing field.

To derive the susceptibilities and spectral densities, cf., Eqs. (10) and (12), we only need to solve the Heisenberg equation for the cavity mode and external field under the free evolution of $\hat{H}_{\rm det}$, according to Ref. [31]:

$$\dot{\hat{a}}(t) = -(\gamma - i\Delta)\hat{a}(t) + \sqrt{2\gamma}\hat{c}_{x=0-}(t)\,, \quad (34)$$

$$\hat{c}_{x=0+}(t) = \hat{c}_{x=0-}(t) - \sqrt{2\gamma}\hat{a}(t)\,, \quad (35)$$

where $\Delta \equiv \omega_l - \omega_r$ is the laser detuning frequency with respect to the cavity resonance. Solving these equations in the frequency domain, we can represent the cavity mode $\hat{a}$ and the outgoing field $\hat{c}_{x=0+}$ in terms of the ingoing field $\hat{c}_{x=0-}$.

Without using the non-classical squeezed light, the spectral density for $\hat{c}_{x=0-}$ is simply $S_{\hat{c}\hat{c}^\dagger}(\omega) = 1$ (vacuum fluctuation) and $S_{\hat{c}^\dagger\hat{c}}(\omega) = 0$, from which we obtain the relevant spectra (double-sided):

$$\bar{S}_{ZZ}(\omega) = \frac{1}{2}, \quad (36)$$

$$\bar{S}_{ZF}(\omega) = \frac{\hbar\bar{g}\sqrt{\gamma}[\Delta\sin\theta - (i\omega - \gamma)\cos\theta]}{(\omega - \Delta + i\gamma)(\omega + \Delta + i\gamma)}\,, \quad (37)$$

$$\bar{S}_{FF}(\omega) = \frac{2\hbar^2\bar{g}^2\gamma(\gamma^2 + \Delta^2 + \omega^2)}{[(\omega - \Delta)^2 + \gamma^2][(\omega + \Delta)^2 + \gamma^2]}\,, \quad (38)$$

and the susceptibilities:

$$\chi_{ZF}(\omega) = -\frac{2\bar{g}\sqrt{\gamma}[\Delta\cos\theta + (i\omega-\gamma)\sin\theta]}{(\omega-\Delta+i\gamma)(\omega+\Delta+i\gamma)}, \tag{39}$$

$$\chi_{FF}(\omega) = \frac{2\hbar\bar{g}^2\Delta}{(\omega-\Delta+i\gamma)(\omega+\Delta+i\gamma)}. \tag{40}$$

One can check that they indeed satisfy the general quantum constraints Eqs. (2) and (3).

For the qubit readout, by introducing $\hat{z} \equiv \hat{Z}/\chi_{ZF}$, we have

$$\hat{z}(\omega) = \hat{z}^{(0)}(\omega) + \hat{\sigma}_z\delta(\omega). \tag{41}$$

Here it uses the fact that $\hat{\sigma}_z$ is a QND observable and remains constant in time. Therefore, the output responds to the signal only near DC with $\omega \approx 0$. For measurement with a finite duration, the delta function $\delta(\omega)$ is approximately equal to the integration time. The measurement rate is defined by the inverse of the integration time that is required to reach signal-to-noise ratio equal to one half, using the convention in Ref. [1]:

$$\Gamma_{\rm meas} \equiv 1/[2\bar{S}_{zz}(0)]. \tag{42}$$

The fluctuation in the cavity photon number induces a random AC Stark shift on the energy level, which causes dephasing, cf., Eq. (31). With measurement much longer than the cavity storage time, only the low-frequency part of the back action noise spectrum is relevant, and according to Ref. [1], the dephasing rate is

$$\Gamma_\phi \equiv (2/\hbar^2)\bar{S}_{FF}(0). \tag{43}$$

At the quantum limit, the ratio between these two rates is given by, cf., Eqs. (2), (37), and (39),

$$\frac{\Gamma_\phi}{\Gamma_{\rm meas}} = 1 + \frac{4\bar{S}_{zF}^2(0)}{\hbar^2} = 1 + \left(\frac{\Delta\sin\theta + \gamma\cos\theta}{\Delta\cos\theta - \gamma\sin\theta}\right)^2. \tag{44}$$

The optimal readout quadrature for reaching $\Gamma_\phi = \Gamma_{\rm meas}$ is therefore the one satisfying

$$\theta_{\rm opt} = -\arctan(\gamma/\Delta). \tag{45}$$

When the cavity is tuned with $\Delta = 0$, $\theta_{\rm opt} = \pm\pi/2$ and the output phase quadrature is the optimal one, cf., Eq. (33), while for a large detuning $\Delta \gg \gamma$, $\theta_{\rm opt} \approx 0$ and we need to measure the output amplitude quadrature. This result can be generalized to more complicated measurement setups with, e.g., multiple coupled cavities. Because such a measurement is near DC and $\bar{S}_{zF}(0)$ is real, we can always find the right readout quadrature such that $\bar{S}_{zF}(0) = 0$, which makes $\Gamma_{\rm meas} = \Gamma_\phi$ at the quantum limit.

We now switch to the case of measuring mechanical motion. In contrast to the qubit readout, the position $\hat{q}_m$ of the mechanical oscillator is not a QND observable, and the back-action noise will appear in the output:

$$\begin{aligned}\hat{z}(\omega) &= \hat{z}^{(0)}(\omega) + \hat{q}_m(\omega)\\ &= \hat{z}^{(0)}(\omega) + \chi_{qq}(\omega)[\hat{F}^{(0)}(\omega) + \hat{F}_{\rm th}(\omega)],\end{aligned} \tag{46}$$

where it uses the fact that $\hat{q}_m = \chi_{qq}[\hat{F}^{(0)} + \hat{F}_{\rm th}]$ with $\hat{F}_{\rm th}$ being the thermal Langevin force and χ_{qq} being the mechanical susceptibility modified by the detector input susceptibility:

$$\chi_{qq}(\omega) = \chi_{qq}^{(0)}(\omega)/[1 - \chi_{qq}^{(0)}(\omega)\chi_{FF}(\omega)], \tag{47}$$

in which $\chi_{qq}^{(0)}$ is the original (bare) mechanical susceptibility. Notice that χ_{FF} is often referred to as the optical spring coefficient or dynamical back action in the literature, which introduces additional heating or damping to the mechanical motion. This has been utilized in the optomechanical sideband cooling experiments [6, 7, 28, 29].

The total output spectrum reads

$$\bar{S}_{zz}^{\rm tot}(\omega) = \bar{S}_{zz}(\omega) + 2\Re[\chi_{qq}^*(\omega)\bar{S}_{zF}(\omega)] + \bar{S}_{qq}(\omega), \tag{48}$$

where $\Re[\cdot]$ means taking the real part. According to Refs. [22, 26], it is the second term, i.e., the cross correlation between the imprecision noise and the back action noise, gives rise to the observed asymmetry. From Eqs. (37) and (39), we have

$$\bar{S}_{zF}(\omega) = -\frac{\hbar}{2}\left[\frac{\Delta\sin\theta - (i\omega-\gamma)\cos\theta}{\Delta\cos\theta + (i\omega-\gamma)\sin\theta}\right]. \tag{49}$$

Those experiments reported in Refs. [21–25] are operating in the resolved sideband regime with the cavity bandwidth much smaller than the mechanical resonant frequency, i.e., $\gamma \ll \omega_m$, and also the detuning frequency $\Delta = \pm\omega_m$. Therefore, near the mechanical resonant frequency ω_m, $\bar{S}_{zF}$ is approximately equal to the one shown in Eq. (5), which leads to

$$2\Re[\chi_{qq}^*(\omega_m)\bar{S}_{zF}(\omega_m)]\big|_{\Delta=\pm\omega_m} \approx \pm\hbar\Im[\chi_{qq}(\omega_m)]. \tag{50}$$

Since $\bar{S}_{qq}(\omega_m) = \hbar(2\langle n\rangle + 1)\Im[\chi_{qq}(\omega_m)]$ with the mean occupation number $\langle n\rangle = 1/(e^{\hbar\omega_m/k_BT} - 1)$ from the fluctuation-dissipation theorem, the above term either doubles or cancels the contribution from the zero-point fluctuation of the mechanical oscillator, which induces the asymmetry. According to Eq. (3), such an imaginary correlation is always associated with the dynamical back action quantified by χ_{FF}:

$$\Im[\chi_{FF}(\omega_m)]_{\Delta=\pm\omega_m} \approx \mp\hbar\bar{g}^2/\gamma \approx \mp\bar{S}_{FF}(\omega_m)/\hbar, \tag{51}$$

as mentioned earlier in Eq. (6).

Before leaving this example, there is one comment motivated by Ref. [34]. The imaginary cross correlation is only detectable near the mechanical resonance when using the homodyne readout, because $\chi_{qq}(\omega_m)$ is also imaginary, which makes the second term in Eq.(48) nonzero. If measuring far away from the resonance or the oscillator were lossless, we will need to apply the synodyne readout scheme presented in Ref. [34] to probe such a quantum correlation.

V. DISCUSSION

The above discussion showed the general quantum constraints for the detector noise in linear continuous measurement. Particularly, the noise spectral densities (quantifying

the quantum fluctuation) and susceptibilities (quantifying the linear response/dissipation) of detectors at the quantum limit were shown to be related by two equalities, which can be viewed as a generalization of the fluctuation-dissipation theorem to the non-equilibrium quantum measurement processes. The result is general and can be applied to different measurement setups, and we have seen two examples in cavity QED.

One last point worthy mentioning is that so far we have only covered linear detectors with single input and single output, which is the case for most experiments mentioned earlier. The result can be generalized to multiple-input-multiple-output (MIMO) detectors through the following identity, which is a generalization of Eq. (29),

$$\det\langle\xi|\hat{\mathbf{A}}(\omega)\hat{\mathbf{A}}^\dagger(\omega')|\xi\rangle = 0\,, \tag{52}$$

where $\hat{\mathbf{A}}^\dagger = (\hat{Z}_1^{(0)}, \hat{F}_1^{(0)}, \cdots, \hat{Z}_N^{(0)}, \hat{F}_N^{(0)})^\dagger$ with N being the number of ports, and the condition of simultaneous measurability:

$$[\hat{Z}_k(t), \hat{Z}_l(t')] = 0 \quad \forall t, t' \tag{53}$$

with $k, l = 1, \cdots, N$. This follows the same logic as deriving the uncertainty relation for MIMO detectors and obtaining Eq. (1) as one special case in Ref. [14].

VI. ACKNOWLEDGEMENT

H.M. would like to thank Farid Khalili and Yanbei Chen for important comments and discussions. This research is supported by EU Marie-Curie Fellowship and UK STFC Ernest Rutherford Fellowship.

[1] A. A. Clerk, M. H. Devoret, S. M. Girvin, F. Marquardt, and R. J. Schoelkopf, Rev. Mod. Phys. **82**, 1155 (2010).
[2] V. Giovannetti, S. Lloyd, and L. Maccone, Nature Photonics **5**, 222 (2011).
[3] E. Jeffrey, D. Sank, J. Y. Mutus, T. C. White, J. Kelly, R. Barends, Y. Chen, Z. Chen, B. Chiaro, A. Dunsworth, A. Megrant, P. J. O'Malley, C. Neill, P. Roushan, A. Vainsencher, J. Wenner, A. N. Cleland, and J. M. Martinis, Phys. Rev. Lett. **112**, 190504 (2014).
[4] S. L. Danilishin and F. Y. Khalili, Living Reviews in Relativity **15** (2012).
[5] R. X. Adhikari, Rev. Mod. Phys. **86**, 121 (2014).
[6] Y. Chen, Journal of Physics B: Atomic, Molecular and Optical Physics **46**, 104001 (2013).
[7] M. Aspelmeyer, T. J. Kippenberg, and F. Marquardt, Rev. Mod. Phys. **86**, 1391 (2014).
[8] K. Jacobs and D. A. Steck, Contemporary Physics **47**, 279 (2006).
[9] H. M. Wiseman and G. J. Milburn, *Quantum Measurement and Control* (Cambridge University Press, 2010) p. 460.
[10] R. Kubo, Reports on Progress in Physics **29**, 255 (1966).
[11] D. V. Averin, Physica C: Superconductivity and its Applications **352**, 120 (2001).
[12] D. V. Averin, arXiv:cond-mat/0301524 (2003).
[13] A. A. Clerk, S. M. Girvin, and A. D. Stone, Phys. Rev. B **67**, 165324 (2003).
[14] V. B. Braginsky and F. Khalilli, *Quantum Measurement* (Cambridge University Press, 1992).
[15] H. B. Callen and T. A. Welton, Phys. Rev. **83**, 34 (1951).
[16] S. Pilgram and M. Büttiker, Phys. Rev. Lett. **89**, 200401 (2002).
[17] J. B. Clark, F. Lecocq, R. W. Simmonds, J. Aumentado, and J. D. Teufel, Nature Physics **12**, 683 (2016).
[18] C. U. Lei, A. J. Weinstein, J. Suh, E. E. Wollman, A. Kronwald, F. Marquardt, A. A. Clerk, and K. C. Schwab, arXiv:1605.08148 (2016).
[19] T. P. Purdy, K. E. Grutter, K. Srinivasan, and J. M. Taylor, arXiv: 1605.05664 (2016).
[20] V. Sudhir, R. Schilling, S. A. Fedorov, H. Schuetz, D. J. Wilson, and T. J. Kippenberg, arXiv:1608.00699 (2016).
[21] A. H. Safavi-Naeini, J. Chan, J. T. Hill, T. P. M. Alegre, A. Krause, and O. Painter, Phys. Rev. Lett. **108**, 033602 (2012).
[22] A. J. Weinstein, C. U. Lei, E. E. Wollman, J. Suh, A. Metelmann, A. A. Clerk, and K. C. Schwab, Physical Review X **4**, 041003 (2014).
[23] T. P. Purdy, P. L. Yu, N. S. Kampel, R. W. Peterson, K. Cicak, R. W. Simmonds, and C. A. Regal, Phys. Rev. A **92**, 031802(R) (2015).
[24] M. Underwood, D. Mason, D. Lee, H. Xu, L. Jiang, A. B. Shkarin, K. Børkje, S. M. Girvin, and J. G. E. Harris, Phys. Rev. A **92**, 061801 (2015).
[25] V. Sudhir, D. J. Wilson, R. Schilling, H. Schütz, S. A. Fedorov, A. H. Ghadimi, A. Nunnenkamp, and T. J. Kippenberg, arXiv:1602.05942 (2016).
[26] F. Khalili, O. Painter, A. Safavi-Naeini, H. Miao, Y. Chen, and H. Yang, Phys. Rev. A **86**, 033840 (2012).
[27] A. Buonanno and Y. Chen, Phys. Rev. D **65**, 042001 (2002).
[28] I. Wilson-Rae, N. Nooshi, W. Zwerger, and T. J. Kippenberg, Phys. Rev. Lett. **99**, 093901 (2007).
[29] F. Marquardt, J. P. Chen, A. A. Clerk, and S. M. Girvin, Phys. Rev. Lett. **99**, 093902 (2007).
[30] K. J. Blow, R. Loudon, S. J. D. Phoenix, and T. J. Shepherd, Phys. Rev. A **42**, 4102 (1990).
[31] C. W. Gardiner and M. J. Collett, Phys. Rev. A **31**, 3761 (1985).
[32] A. Blais, R. S. Huang, A. Wallraff, S. M. Girvin, and R. J. Schoelkopf, Phys. Rev. A **69**, 062320 (2004).
[33] A. Wallraff, D. I. Schuster, A. Blais, L. Frunzio, J. Majer, M. H. Devoret, S. M. Girvin, and R. J. Schoelkopf, Phys. Rev. Lett. **95**, 060501 (2005).
[34] L. F. Buchmann, S. Schreppler, J. Kohler, N. Spethmann, and D. M. Stamper-Kurn, Phys. Rev. Lett. **117**, 030801 (2016).